



OPEN ACCESS

EDITED BY Qing-Wei Wang. Chinese Academy of Sciences (CAS), China

REVIEWED BY Xiaovu Wang Zhejiang Agriculture and Forestry University, China Zhengbing Yan, Chinese Academy of Sciences (CAS), China

Lahcen Benomar □ lahcen.benomar@ontario.ca

RECEIVED 12 June 2025 ACCEPTED 22 September 2025 PUBLISHED 22 October 2025

Benomar L, Elferjani R and Lu P (2025) Functional trait recovery through backcross breeding in blister rust-resistant hybrid white pines (Pinus strobus × Pinus wallichiana). Front. For. Glob. Change 8:1645556. doi: 10.3389/ffgc.2025.1645556

© 2025 Benomar, Elferjani and Lu. This is an open-access article distributed under the terms of the Creative Commons Attribution License (CC BY). The use, distribution or reproduction in other forums is permitted, provided the original author(s) and the copyright owner(s) are credited and that the original publication in this journal is cited, in accordance with accepted academic practice. No use, distribution or reproduction is permitted which does not comply with these terms.

Functional trait recovery through backcross breeding in blister rust-resistant hybrid white pines (Pinus strobus × Pinus wallichiana)

Lahcen Benomar^{1*}, Raed Elferjani² and Pengxin Lu¹

¹Ontario Forest Research Institute, Ontario Ministry of Natural Resources, Sault Ste. Marie, ON, Canada, ²Independent Researcher, Trois-Rivieres, QC, Canada

Introduction: White pine blister rust (WPBR) disease, caused by an invasive fungal pathogen (Cronartium ribicola J.C. Fisch), has long been the primary biotic threat to eastern white pine in Canada. A hybridization program initiated in Ontario, Canada in the 1950s aimed to transfer blister rust resistance from Himalayan blue pine to eastern white pine, resulting in WPBR-resistant interspecific hybrids. Metabolic adjustments related to disease resistance may cause trade-offs with tolerance to abiotic stress (e.g., frost, heat, drought). To evaluate the adaptive potential of WPBR-resistant hybrids, it is crucial to understand how morphological and physiological traits change during multigeneration backcrossing, as these shifts may influence both growth performance and resilience to climate change.

Methods: We assessed changes in photosynthetic-related traits, as well as needle morphology and resistance to xylem cavitation of eastern white pine and Himalayan blue pine, and their hybrids with varying levels of white pine parentage ranging from 50 to 87.5%.

Results and discussion: Needle length and specific leaf area (SLA) decreased linearly by increasing eastern white pine parentage; inversely, needle density increased by increasing eastern white pine parentage. Variations in needle morphology were not translated into variations in light-saturated photosynthesis (Amax), mesophyll conductance (g_m) , maximum rate of carboxylation (V_{cmax}) , and maximum rate of electron transport (J_{max}). Photosynthetic nitrogen use efficiency (PNUE) decreased, while water use efficiency (WUE) increased with increasing eastern white pine parentage. Increasing needle density and declining PNUE reflect greater investment in structural tissue, which is commonly associated with frost and drought tolerance. Also, Himalayan blue pine and hybrids were more resistant to xylem cavitation than eastern white pine. Hybrid pines recovered most of their eastern white pine morpho-physiological characteristics after two rounds of backcrossing. Consequently, WPBR-resistant interspecific hybrids should have integrated stress tolerance traits of eastern white pine enabling them to adapt to abiotic and biotic stresses in Canadian boreal forests.

tree breeding, stomatal density, needle length, photosynthetic rate, xylem embolism, hydraulic safety margin, photosynthetic nitrogen use efficiency (PNUE), water use efficiency (WUE)

Introduction

Eastern white pine (Pinus strobus L.) is a coniferous tree species native to eastern North America (Wendel and Smith, 1990). The species, which has undergone a severe decline in the last century, is a keystone tree prized for its ecological, economic, and cultural significance (Parker, 2008; Wendel and Smith, 1990). Unsuccessful regeneration contributes to the decline of the eastern white pine across its natural range in Canada and the United States. White pine blister rust (WPBR), a disease caused by an invasive fungal pathogen, Cronartium ribicola J.C. Fisch, is considered the predominant threat to white pine regeneration (Pitt et al., 2006; Spaulding, 1922). The low resistance of eastern white pine to WPBR limits efforts of overcoming the disease using traditional intraspecific breeding strategies (Heimburger, 1962; Heimburger, 1972; Lu et al., 2005; Lu and Derbowka, 2009). Transferring WPBR resistance from Eurasian white pine species to eastern white pine through hybridization was a promising alternative strategy used in Ontario, Canada (Lu and Derbowka, 2009; Heimburger, 1972; Blada, 2004). The hybridization of eastern white pine with resistant and compatible Eurasian five needle pines resulted in strongly resistant interspecific hybrids (Lu and Derbowka, 2009; Lu et al., 2005; Lu and Sinclair, 2006; Patton, 1966). In Ontario, Canada, breeding eastern white pine and Himalaya blue pine (Pinus walichiana) for interspecific hybrids has advanced to the second-generation backcross (BC2F1) with highly resistant families (Lu and Derbowka, 2009).

Hybrid pines can exhibit combinations of physiological traits of both parents or be more similar to one parent (Lilly et al., 2012; Houminer et al., 2022; Keng et al., 1961), which shapes the hybrids' response to biotic and abiotic factors. When grown at different locations in Ontario, Himalayan blue pine × eastern white pine hybrids had similar or greater height growth rates than their parents (Lu and Sinclair, 2006). However, the F1 hybrids were sensitive to frost, which limited their survival in northern sites (Lu and Sinclair, 2006; Patton, 1966). Frost tolerance improved in backcrosses to eastern white pine (Lu and Sinclair, 2006; Lu et al., 2007).

As eastern white pine hybrid breeding continues for blister rust resistance, Ontario has produced different levels of eastern white pine hybrid backcrosses. Understanding how morphological and physiological traits have changed throughout the backcrossing process is needed to assess effects on growth performance of future breeding products under different site conditions and, consequently, their adaptive capacity to climate change.

Needle size is key to tree growth and adaptation through its effect on light interception efficiency, CO_2 assimilation capacity, and transpiration rate. Five-needle pines exhibit a noticeable difference in needle length ranging from 05 to 50 cm (Keng et al., 1961; Wang et al., 2019), and their F1 hybrids often have needles with intermediate lengths, compared to their parents (Keng et al., 1961). The effect of changed needle length during hybridization on needle physiology is still unknown but could lead to changes in morphology, anatomy, and physiology. Previous studies showed that needle length decreases with a decreasing mean winter minimum temperature (Jankowski et al., 2017; Reich et al., 2003; Nobis et al., 2012). Increased needle length may be associated with increased specific leaf area (SLA) and, inversely, decreased needle density (i.e., needle dry mass per unit area) (Wang et al., 2019; Jankowski et al., 2017). Several studies have revealed a negative association between SLA and frost tolerance

(Poorter et al., 2009; Niinemets, 2001; Niinemets, 2016; Rajashekar and Burke, 1996). As such, a change in needle length may shift the nitrogen fraction allocated to cell walls and light harvesting and, consequently, alter drought and frost tolerance. Decreased needle density and increased needle length mean more investment of needle nitrogen in photosynthetic machinery, which may result in a rise in the carboxylation rate and electron transfer capacity (Onoda et al., 2017; Niinemets and Tenhunen, 1997). Also, a decrease in needle density may increase the conductance of CO₂ movement through mesophyll from the intercellular air space to the sites of carboxylation in chloroplasts (Evans, 2021; Flexas et al., 2013), with a positive effect on CO2 assimilation rate. However, this effect may depend on the magnitude of change in needle density. Mesophyll conductance of needles is also influenced by hydraulic conductance which scaled with needle length in pine species (Wang et al., 2019). One may therefore expect increased needle mesophyll conductance and CO₂ assimilation rate in longer needles. Five-needle pine F1 hybrids produced needles with an intermediate or similar number of stomatal rows as their parents (Keng et al., 1961). This may affect needle stomatal density and potentially stomatal conductance and water use efficiency of hybrid pines, being different from their parents. It is thus crucial to know if trade-offs exist between blister rust resistance and resource use efficiency among parents and their hybrids due to changes in needle length. In conifers, a trade-off exists between xylem's capacity to transport water and its susceptibility to cavitation. This balance is highlighted by the negative correlation between wood density and vulnerability to cavitation (P50) (Hacke et al., 2015; Rosner, 2017). Lu and Sinclair (2006) found that the Himalayan blue pine has a higher wood density than eastern white pine while their hybrids have intermediate densities, suggesting that hybrid pines may have lower P50 and better drought tolerance compared to the eastern white pine.

While prior studies have documented WPBR resistance, growth performance, and frost tolerance in white pine hybrids, this research represents the first study to examine how needle morphology, physiological traits, and xylem resistance to cavitation evolve through successive backcross generations. We propose that (i) according to the leaf coordination theory, changes in needle morphology and physiology are associated with changes in needle length, reflecting shifts in traits such as specific leaf area (*SLA*), needle density, and stomatal distribution; (ii) the backcrossing process effectively recovers eastern white pine traits, such that hybrid trait expression is shaped by the degree of eastern white pine parentage; and (iii) the enhanced wood density noted for Himalayan blue pine and its hybrids (Lu and Sinclair, 2006) will provide greater resistance to xylem cavitation (P50) in hybrids compared to eastern white pine.

Materials and methods

Genetic material

We collected needle samples from three white pine genetic archives established in Sault Ste. Marie, ON, Canada, between 1995 and 2011. The archives were established on abandoned agricultural land with loam-sandy, well-drained soil. The soil was scarified before planting, and trees were planted with 3.0×3.0 m spacing using

potted grafted clonal stock. Trees of the same families were planted together, with 3 to 6 individuals per family. The genetic material used in this study consisted of four clones of Himalayan blue pine (Pinus wallichiana), six clones of eastern white pine, and 21 hybrid families which had varying levels of P. strobus parentage, ranging from 50 to 87.5% (see Table 1). Notably, the selected hybrid pine families were found to be highly resistant to blister rust in experiments with artificial inoculation of Cronartium ribicola (Lu et al., 2005). In the initial F₁ hybrids, P. wallichiana trees served as the maternal parents, while the pollen donor was *P. strobus* trees. The *P. wallichiana* parents were sourced from 17 different provenances across Pakistan (Lu and Sinclair, 2006). In successive backcrossings, either hybrid trees were pollinated with eastern white pine pollen or eastern white pine trees were pollinated with pollen from hybrid trees (Lu and Derbowka, 2009). Since the breeding process was designed to produce hybrid progeny with high level of genetic diversity of eastern white pine genome in the BC1 and BC2 generations, this study was thus not limited to observe progeny from fixed numbers of male or female parents; rather, it aimed to detect morphological and physiological differences among broad genotype groups represented by P. strobus parentage.

The 31 families were randomly selected from existing families in the three archives (refer to Table 1). To assess the vulnerability of the xylem to cavitation, two individuals from each family were chosen, and family mean values were used later for statistical analysis. However, for all other measurements, only 21 out of the 31 families were included, with each family represented by just one individual tree (Table 1).

Stomatal density

For each tree in the 21 selected families (Table 1), three branches were collected from the sun-exposed part of the trees, transported on ice in a cooler, and stored in a refrigerator until analysis. A subsample of three fascicles was used for stomatal density measurements, and the rest was used for needle morphology.

Needles were flattened, taped on both extremities, and photographed with a USB microscope (Dino-Lite digital 5mp, Electronics Corp., Taipei, Taiwan). The central part of the needle was photographed to avoid any

TABLE 1 Selected families utilized for the morpho-physiological characterization of eastern white pine (*P. strobus*) and Himalayan blue pine (*P. wallichiana*) and their interspecific hybrids with varying eastern white pine parentage.

Species	<i>P. strobus</i> parentage (%)	Number of selected families	Plantation date
P. wallichiana (w)	0	4(4)	1995
wxs	50	4(5)	1995
(w x s) x (w x s)	50	(2)	1995
(w x s) x s	75	4(7)	2006
((w x s) x (w x s)) x s	75	1(1)	2006
((s x w) x s) x s	87.5	4(6)	2011, 2006
P. strobus (s)	100	4(6)	2011,1995

The number in parentheses indicates the number of families used for xylem vulnerability to cavitation measurements.

potential variation at the extremities. Abaxial and adaxial needle surfaces were photographed in each sample at a magnification of $230 \times (\text{Figure 1})$. Five-needle pine needles have a triangular shape (three sides) with stomata present only on the two abaxial sides (Ghimire et al., 2015), from which we determined the number of stomata and stomata rows. Stomata were counted along the 1 mm needle length in magnified images using the line measure tool in the DinoCapture 2.0 software (Figure 1) from each of the two abaxial sides. Stomatal density was calculated as the number of stomata within 1 mm of both sides of the needle multiplied by needle length (mm) divided by the projected needle area (mm²).

Needle morphology and N-P-K concentrations

Needle fascicles were disarticulated and then placed on a flatbed scanner. Needle length, width, and projected area were then measured using WinSeedle (Version 2007 Pro, Regent Instruments, Québec, Canada). Needle samples were then oven-dried for 72 h at 56 °C, and their dry mass weighed. Specific leaf area (SLA) was calculated as the ratio of the projected needle area (cm^2) to needle dry mass (g). Dried needles were grounded into a fine powder in a ball mill to determine needle nitrogen (N_{mass}), phosphate (P_{mass}) and potassium (K_{mass}) concentrations ($cmg g^{-1}$) using a LECO elemental analyzer (Leco Corporation, St-Joseph, Michigan). Nitrogen ($cmg g^{-1}$) and potassium ($cmg g^{-1}$) were calculated on a projected area basis as $cmg g^{-1}$ were calculated on a projected area basis as $cmg g^{-1}$

Needle water potential

Predawn (Ψ_{nd}) and mid-day (Ψ_{md}) needle water potential was assessed in two consecutive growing seasons (2023 and 2024) using a pressure chamber (model 610, PMS Instruments, Albany, OR, USA). The same families were later used for needle morphology and gas exchange measurements. The Ψ_{md} was measured in July and August as the dry and wet period, respectively. Soil volumetric water content (VWC) and weather conditions were monitored during each period to select the driest day in July and the wettest day in August. The Ψ_{pd} measurements were carried out only on July 10, 2023. Three sunny branches with one-year-old needles were cut and immediately sealed in zipped plastic bags containing a dampened paper towel and stored in an ice cooler (Rodriguez-Dominguez et al., 2022). Branches were collected before sunrise between 04:30 and 06:00 a.m. for Ψ_{pd} and between 12:30 and 02:30 p.m. for Ψ_{md} . The mid-day water potential during the driest period was considered as the minimum leaf water potential (Ψ_{min}). For each tree, water potential was measured on three separate fascicles from three different branches, and the mean value was used for statistical analysis. An additional needle fascicle was measured if the original three samples differed by more than 0.2 MPa. To avoid any post-excision transpiration-driven water potential disequilibrium, sampled needles were allowed to reach equilibrium for at least 2 h and measured within 24 h after sampling (Rodriguez-Dominguez et al., 2022). The pressure chamber was humidified by placing a humid paper towel at the bottom. The soil's volumetric water content (VWC) was measured on the day of branch collection using time-domain reflectometry. The measurements were taken at 20 cm depth in three spots within a 1 m radius of the stem of the targeted tree (Figure 2).

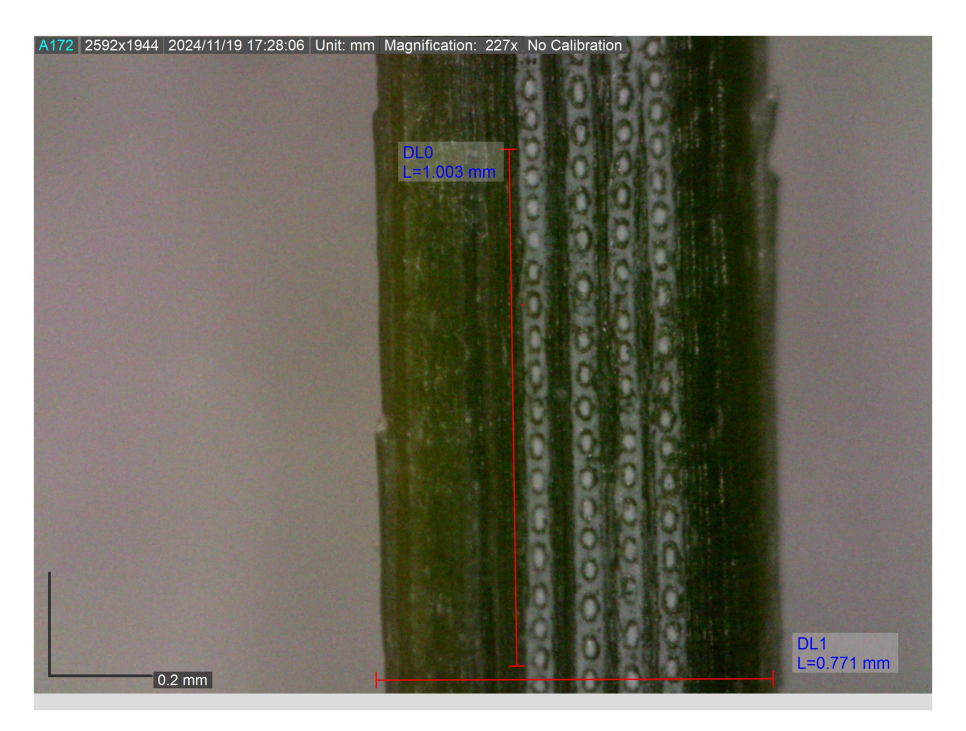


FIGURE 1
Magnified images (230x) of eastern white pine needle abaxial surfaces. The image was taken at the center of the needle and shows the four stomata rows. The stomatal density was determined based on the number of stomata along the 1 mm segment (DL0) of the needle length. DL1 needle diameter, width and, length measurements are shown on photographs of abaxial leaf surface.

Curve of vulnerability of the xylem to cavitation

Branches on the sunny side of the crown were collected from each of the 31 selected families (Table 1) using a pole pruner in June 2023. Two to four branch samples were collected for each family from straight 50 cm long branches with a 1-1.5 cm diameter which resulted in 95 samples. Straight branch segments were collected in the early morning (08:00 to 10:00 a.m.) to minimize xylem tension and immediately wrapped in wet paper towels and plastic bags and stored in the cooler before being shipped the same day to the CaviPlace laboratory at the University of Bordeaux in France. 1 The samples arrived 4 days later and were kept at 5 °C until hydraulic attributes were measured. The measurements were carried out within 2 weeks after sample collection. Prior to measurement, branches were cut under water with a razor blade to a standard length of 27 cm. The bark was removed, and the branches were fully rehydrated before further processing. The vulnerability of the xylem to cavitation was measured with the Cavitron technique, which uses the centrifugal force to generate a negative pressure into the xylem and measure its hydraulic conductance under such pressure conditions to generate the vulnerability curve as described in Cochard et al. (2005). Xylem conductance was measured first at a reference pressure of -0.8 MPa, and the maximal hydraulic conductivity (K_{max} in m² MPa⁻¹ s⁻¹) was determined. Thereafter, xylem pressure was changed gradually to more negative pressures in 0.5 MPa increments, and the hydraulic conductivity, K, was measured at each step. Data acquisition and processing were performed using the Cavisoft software (Cavisoft v1.5, University of Bordeaux, Bordeaux, France). The vulnerability curves were fit with the following sigmoid function (Pammenter and Van der Willigen, 1998):

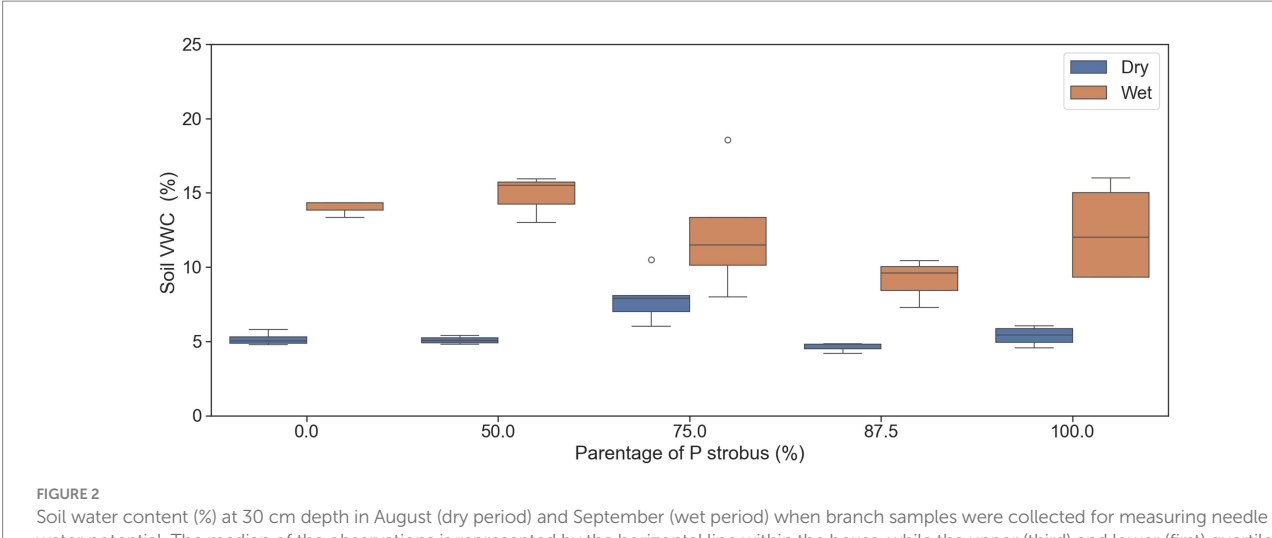
$$PLC = \frac{100}{\left[1 + \exp^{\left(\frac{S}{25}(P - P50)\right)}\right]}$$

where PLC is the percentage loss in hydraulic conductivity; S is the negative slope (% MPa⁻¹) of the vulnerability curve at the inflection point; P50 (MPa), cavitation resistance, is the xylem pressure inducing 50% loss of xylem hydraulic conductance. The vulnerability curve slope (S) is a good indicator of the speed at which embolisms affect the stem (Delzon and Cochard, 2014; Delzon et al., 2010). The hydraulic safety margin was calculated as the difference between $\Psi_{\rm min}$ and P50 (Delzon and Cochard, 2014; Klein et al., 2014).

Needles gas exchange

Needle-level gas exchange was measured using a portable openpath gas-exchange system (Li-6400, Li-Cor Inc., Lincoln NE) equipped with a lighted 2×3 cm broadleaf chamber (Li-6400-40, Li-Cor Inc). The measurements were carried out using one-year-old needles of excised sunny branches on the same trees used for water

¹ http://sylvain-delzon.com/caviplace



Soil water content (%) at 30 cm depth in August (dry period) and September (wet period) when branch samples were collected for measuring needle water potential. The median of the observations is represented by the horizontal line within the boxes, while the upper (third) and lower (first) quartiles of the value ranges are indicated by the box ends.

potential and needle morphology measurements. Branches were cut, immediately plunged in water, and the lower 2 cm cut under water and put in water-filled plastic tubes until the end of gas exchange measurements. Several studies showed the efficacy of excised branches for gas exchange measurement on conifer species (Dang et al., 1997; Ethier et al., 2006). Additionally, before measurements, we tested three separate branches, which showed that the excised branch maintains the same CO2 assimilation and stomatal conductance 3 h after excision, and if put in dark conditions immediately after collection, 24 h. We flattened seven fascicles attached to the main twig for each sample and inserted them in the cuvette area. We measured the photosynthetic CO₂ response curve (A-Ci) after 30 min of steady-state conditions within the cuvette. The flow, temperature, vapor pressure deficit (VPD), CO₂ (Ca, inside the cuvette), and photosynthetic active radiation (PAR) inside the cuvette were maintained at 300 μ mol s⁻¹, 20 \pm 1 °C, 1 \pm 0.2 kPa, 415 μ mol mol $^{-1}$, and 1,500 μ mol m $^{-2}$ s $^{-1}$, respectively. The saturation PAR was determined based on three photosynthetic light response curve (A-Q) measurements per white pine parentage (Supplementary Figure S1). Thereafter, C_a (CO₂ inside the cuvette) was changed in the following order: C_a : 415, 400, 350, 300, 250, 200, 150, 100, 50, 415, 500, 550, 600, 650, 700, 800, 900, 1,000, 1,100, 1,200, 1,400, and 1,500, 1800 µmol mol-1. Values were recorded based on the stability of photosynthetic assimilation rate (A_{max}) and stomatal conductance to water (g_{sw}) . The attachment points of the needles to cuvette walls were taped using the plasticine, allowing easy placement of needles and avoiding leaks in and out of the cuvette. Therefore, data were not corrected for CO2 leaks. Intrinsic water use efficiency (WUEi) was calculated as A_{max} at ambient CO₂ divided by stomatal conductance to water (g_{sw}) . Photosynthetic nitrogen use efficiency (PNUE) was calculated as A_{max} divided by N_{area} .

Estimation of gas exchange parameters

Mesophyll conductance (g_m , CO_2 transfer conductance from the intercellular space to the sites of carboxylation in chloroplasts), the

maximum rate of carboxylation (V_{cmax} , μ mol CO₂ m⁻² s⁻¹), and the maximum rate of electron transport (J_{max} , μ mol m⁻² s⁻¹) were estimated simultaneously from the A-Ci response curves. After (Ethier and Livingston, 2004; Niinemets et al., 2004), A-Ci curves were fit with the non-rectangular hyperbola version of the biochemical C₃ photosynthesis model (Farquhar et al., 1980) using nonlinear regression techniques (Proc Nlin, SAS) as described in Sun et al. (2014). J_{max} was assumed to equal J at light saturation (Long and Bernacchi, 2003).

Statistical analyses

Statistical analyses were performed with Python version 3.9. The effect of water moisture and genotype and their interaction on needle mid-day water potential was analyzed using a two-way ANOVA. P50, the slope of the curve of the vulnerability to cavitation, needle morphological traits (SLA, needle density, needle length and width, stomatal rows, stomatal density) and photosynthetic-related traits ($A_{max}, g_{sw}, V_{cmax}, J_{max}$) J_{max} : V_{cmax} , g_m , SLA, N_{mass} , P_{area} , K_{area} , N_{area} , PNUE, WUE_i) were compared between pines and hybrids using one-way analysis of variance with the Statsmodels package (0.11.1). Family means were used as observations in ANOVAs and adjusted Tukey tests (HSD) were used to determine statistical significance among species and hybrids in those traits. Nonparametric one-way ANOVAs were used when ANOVA assumptions, such as homogeneity of variance and normality of residuals, were not met even after transformation (stomatal density, WUE_i). Spearman correlations were used to examine the correlation between xylem and needle functional traits. Correlations were considered significant at $p \le 0.05$.

Results

Needle morphological characteristics

Needles were 8 to 14 cm long, with Himalayan blue pine having the longest needles, followed by hybrids then eastern white pine. Needle

length decreased linearly as eastern white pine parentage increased $(p = 0.002; R^2 = 0.97;$ Figure 3). Conversely, needle width had no relationship with eastern white pine parentage (p = 0.62; $R^2 = 0.06$; Figure 3). Like needle length, specific leaf area (SLA) was the largest for blue pine and decreased linearly as eastern white pine parentage increased $(p = 0.04; R^2 = 0.79; Figure 3)$. Needle density (NeD, g cm⁻³) was lowest for blue pine and increased linearly as eastern white pine parentage increased (p = 0.003; $R^2 = 0.94$; Figure 3). The highest number of stomatal rows on both sides of the needle surfaces was observed in blue pine, followed by eastern white pine and its hybrids with 50 and 75% eastern white pine parentage. The hybrids with 87.5% eastern white pine parentage had the fewest stomatal rows. Also, there was no variation in stomatal rows among eastern white pine families, which consistently showed 3 and 4 rows on the two abaxial sides, as well as among hybrids with 50 and 75% eastern white pine parentage. However, stomatal rows did differ among blue pine families, which had 5-6 or 4-5 rows, and hybrids with 87.5% eastern white pine parentage, which had 3-2 or 3-4 rows (Table 2). Stomatal density was, however, similar between species and hybrids (Table 2). Nitrogen on a projected area basis (N_{area}) was lowest for blue pine and increased linearly as eastern white pine parentage increased (p = 0.048; $R^2 = 0.77$). In contrast, the potassium (K_{area}) and phosphorus (P_{area}) on a projected area basis were similar among parent pine species and hybrids (Table 2).

Needle water potential and xylem embolism

Midday needle water potential (Ψ_{md}) was affected by soil water content (p=0.001) but not by species (p=0.392), and no significant interaction between soil moisture and species was found (p=0.90). The Ψ_{md} was lower during the dry period (low volumetric water content) than the wet period in the growing season. Regardless of sampling period, Ψ_{md}

was similar among hybrids and the two pine species (Figure 4). The predawn water potential (Ψpd), measured only during the dry period, was similar between pines and hybrids (p=0.16; Figure 4). P50 of the vulnerability curve was 10% lower for eastern white pine than blue pine and hybrids (p=0.007; Figure 5). However, the slopes of the vulnerability curves were similar for pine species and their hybrids (p=0.058). The hydraulic safety margin was the lowest for eastern white pine (p=0.001; Figure 5).

Needle gas exchange

Light-saturated photosynthesis (A_{max}) was not significantly different between species and hybrids (p = 0.062), stomatal conductance (g_{sw}) was higher (0.109 mol H₂O m⁻² s⁻¹) in blue pine than eastern white pine and hybrids containing 87.5% eastern white pine parentage (0.064 to 0.065 mol CO₂ m⁻² s⁻¹), while hybrids containing 50 and 75% of eastern white pine parentage had intermediate values. Like A_{max} , mesophyll conductance (g_m , mol CO₂ m⁻² s⁻¹), the maximum rate of carboxylation (V_{cmax} , µmol CO₂ m⁻² s⁻¹), the maximum rate of electron transport (J_{max} , µmol m⁻² s⁻¹), and the J_{max} : V_{cmax} ratio were similar among pines and hybrids (Table 2). Intrinsic water use efficiency (WUE_i) was highest for eastern white pine and decreased linearly as eastern white pine parentage decreased (p = 0.007; $R^2 = 0.96$; Figure 6). In contrast, photosynthetic nitrogen use efficiency (PNUE) was the highest for the blue pine and decreased linearly as eastern white pine parentage increased (p = 0.014; $R^2 = 0.90$; Figure 6).

Functional relationships

Needle length was positively correlated with SLA while Needle density was negatively correlated with N_{area} and SLA (Figure 7). SLA

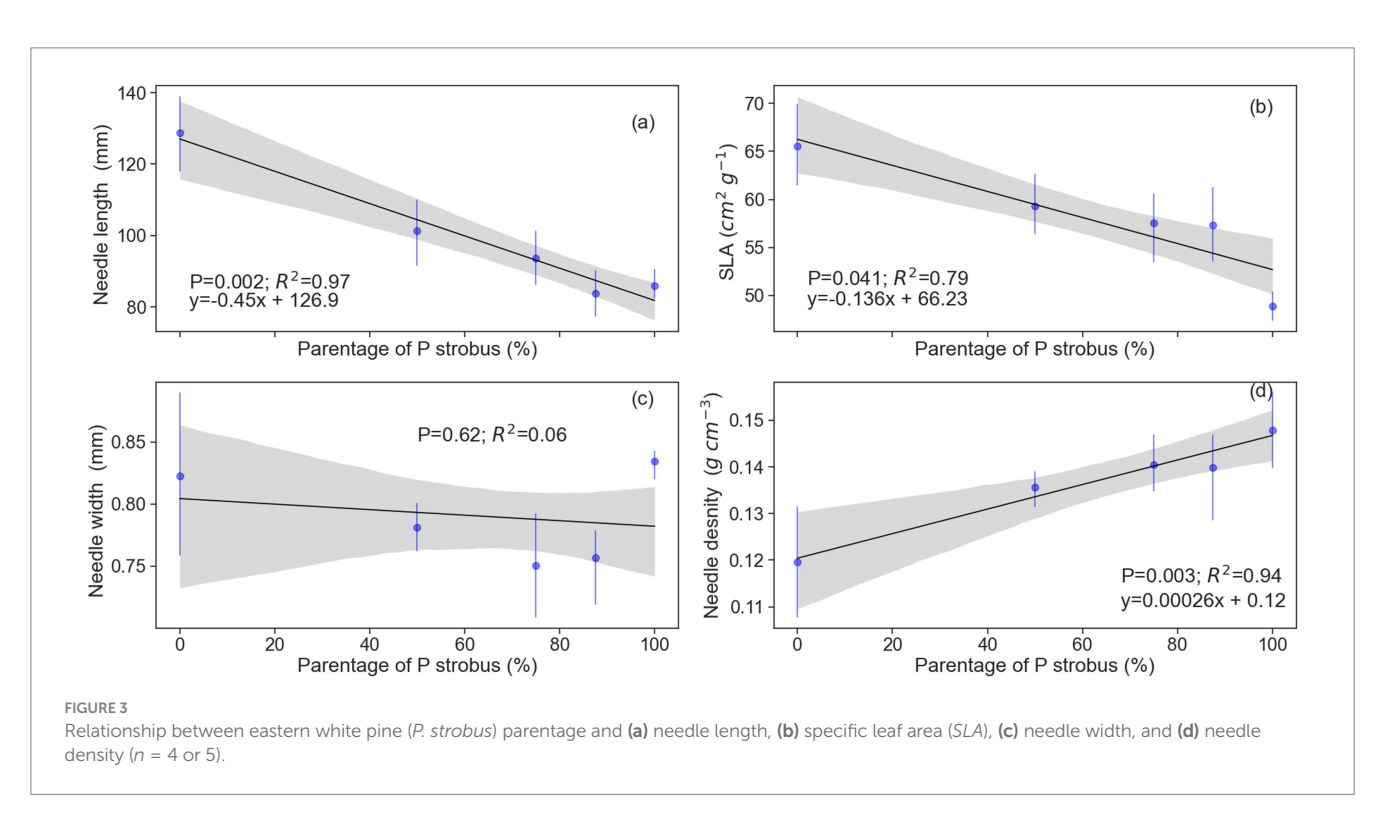
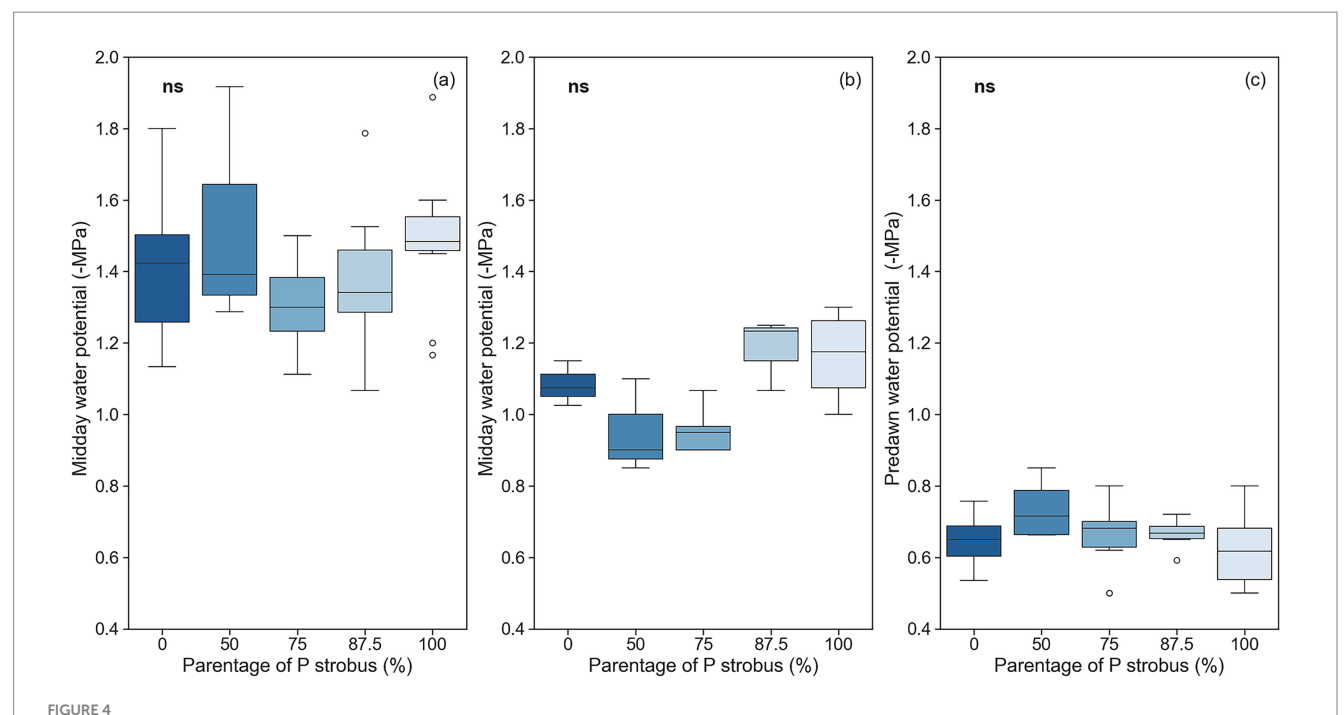


TABLE 2 Needles morpho-physiology traits of eastern white pine (P. strobus) and Himalayan blue pine (P. wallichiana) and their interspecific hybrids with varying eastern white pine parentage (mean \pm std).

Trait	P. strobus Parentage %					
	0%	50%	75%	87.5%	100%	
Stomata rows	5-6/5-4	3–4	3-4	3-4/2-3	3-4	
Stomata density (No mm ⁻²)	204 ± 43a	176 ± 51a	199 ± 33a	141 ± 18a	147 ± 10a	
A_{max}	9.6 ± 1.3a	7.7 ± 1.8a	8.6 ± 1.8a	6.8 ± 0.4a	8.1 ± 1.0a	
g _{sw}	0.119 ± 0.02a	0.078 ± 0.02ab	0.085 ± 0.03ab	0.064 ± 0.01b	0.065 ± 0.01b	
g_m	0.109 ± 0.02a	0.071 ± 0.02a	0.098 ± 0.02a	0.082 ± 0.01a	0.092 ± 0.01a	
V_{cmax}	32.8 ± 4.3a	34.8 ± 9.8a	35.4 ± 4.4a	34.9 ± 9.7a	36.3 ± 15.4a	
J_{max}	73.9 ± 8.2a	75.6 ± 20.5a	76.2 ± 10.5a	73.2 ± 16.9a	80.7 ± 23.5a	
J _{max} : V _{cmax}	2.2 ± 0.1a	2.1 ± 0.1a	2.1 ± 0.1a	2.1 ± 0.1a	2.1 ± 0.1a	
N _{area}	2.24 ± 0.29b	2.61 ± 0.23b	2.86 ± 0.47ab	2.78 ± 0.22ab	3.59 ± 0.52a	
K _{area}	0.56 ± 0.05a	$0.63 \pm 0.05a$	0.65 ± 0.14a	0.60 ± 0.11a	0.72 ± 0.11a	
P_{area}	0.21 ± 0.03a	0.24 ± 0.02a	0.23 ± 0.04a	0.25 ± 0.05a	0.28 ± 0.03a	

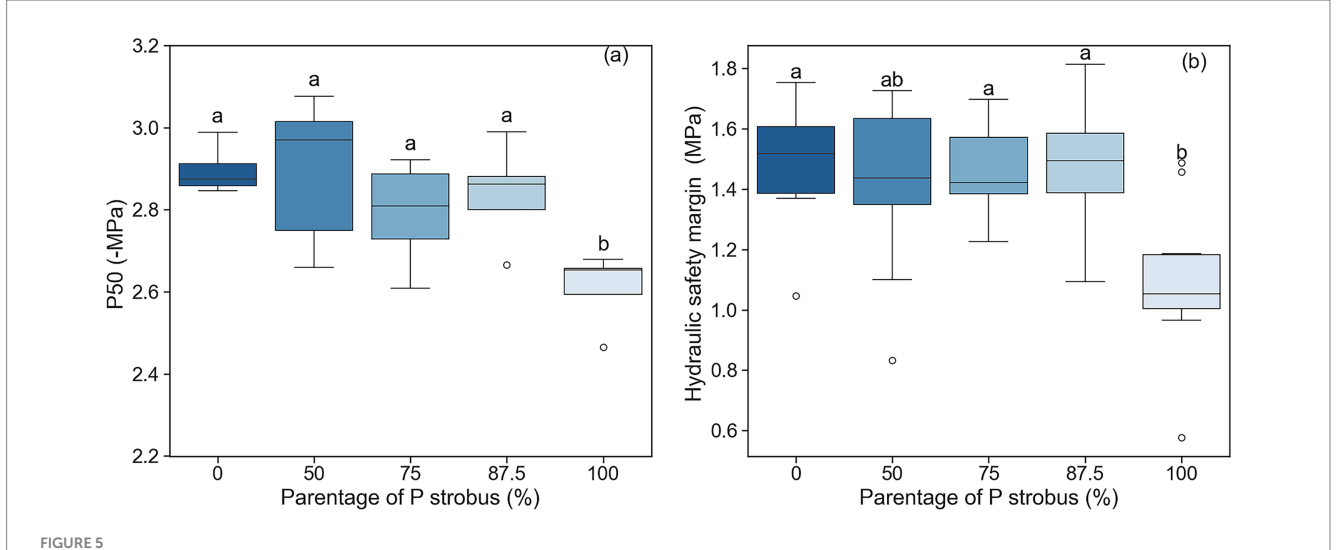
 A_{max} light-saturated photosynthetic rate (µmol CO₂ m⁻² s⁻¹); g_{mo} stomatal conductance for water (mol H₂O m⁻² s⁻¹); g_{mv} mesophyll conductance (mol CO₂ m⁻² s⁻¹); V_{cmax} the maximum rate of carboxylation (µmol CO₂ m⁻² s⁻¹); J_{max} the rate of electron transport (µmol CO₂ m⁻² s⁻¹); J_{max} . V_{cmax} The ratio of J_{max} to V_{cmax} . Leaf nitrogen in area basis (g m⁻²); K_{avea} . Leaf nitrogen in area basis (g m⁻²); V_{cmax} Lea



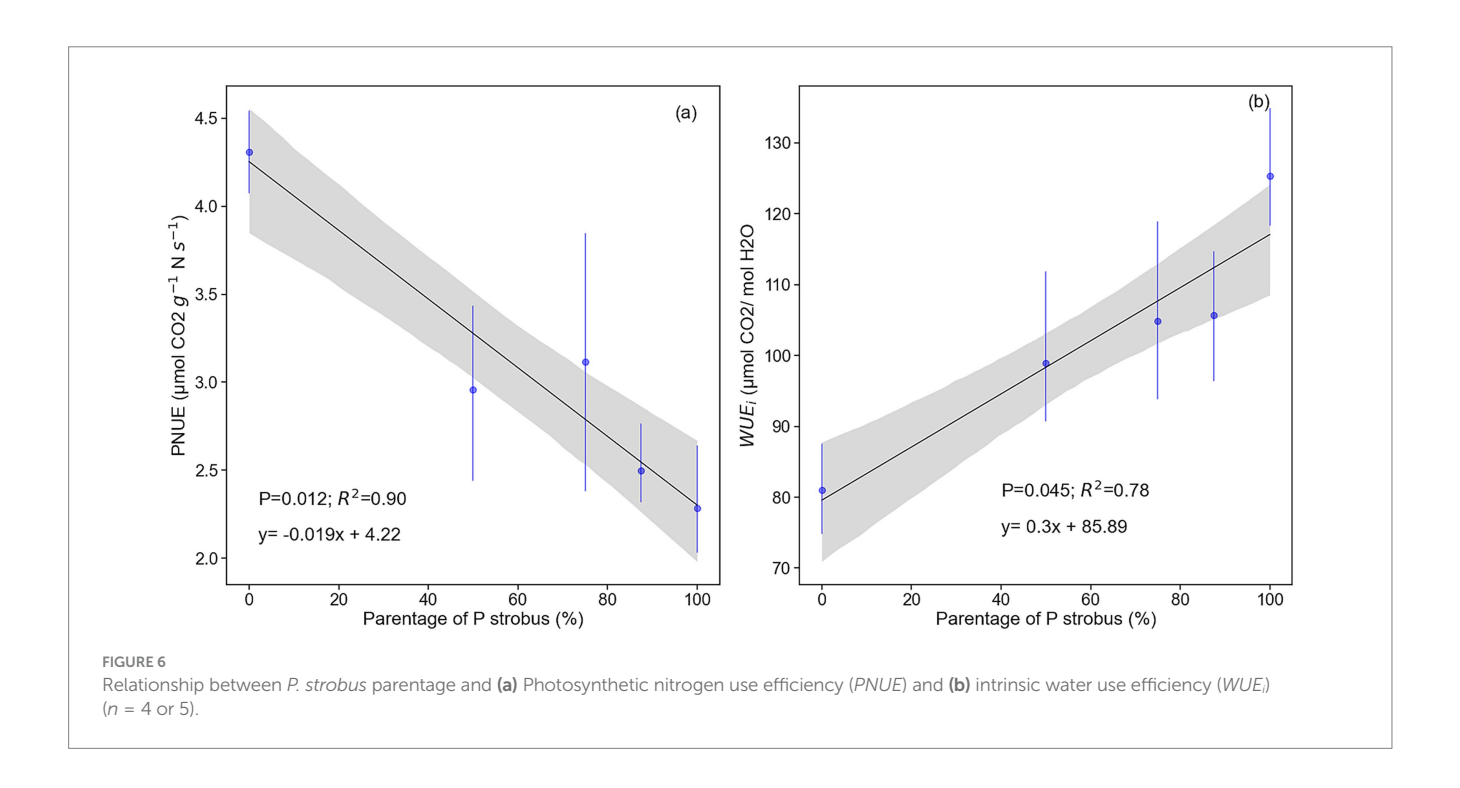
Needle water potential of eastern white pine (P. strobus) and Himalayan blue pine (P. wallichiana) and their interspecific hybrids with varying eastern white pine parentage: (a) midday water potential in dry period, (b) midday water potential in wet period, and (c) predawn water potential in dry period. The median of the observations is represented by the horizontal line within the boxes, while the upper (third) and lower (first) quartiles of the value ranges are indicated by the box ends. Means with the same letters are not significantly different at $\alpha = 0.05$ (n = 4 to 5). n = 4 NOVA test not significant.

was negatively correlated with N_{area} , WUE_i and J_{max} and positively with xylem hydraulic safety margin (HSM) (Figure 7). Stomatal density was positively correlated to g_{sw} (Figure 7). As for photosynthesis-related traits, A_{max} was related to its CO_2 diffusion limitations (g_{sw} and g_m), but not to its biochemical limitations (V_{cmax} and V_{cmax}) (Figure 7). Stomatal conductance and mesophyll conductance were unrelated. Unexpectedly, V_{cmax} and V_{cmax} were also unrelated (Figure 7). V_{cmax} was

negatively correlated with SLA and positively with needle density, N_{area} and the ratio between mesophyll conductance and stomatal conductance (g_{sw},g_m) (Figure 7). Photosynthetic nitrogen-use efficiency was negatively correlated with WUE_i and positively with SLA and g_{sw} (Figure 7). Predawn and midday water potential were unrelated, and both were unrelated with P50 and xylem P50 and P50 (Figure 7).



(a) Cavitation resistance (P50), (b) hydraulic safety margin of eastern white pine (P.Strobus) and Himalayan blue pine (P.Strobus) and their interspecific hybrids with varying eastern white pine parentage. The median of the observations is represented by the horizontal line within the boxes, while the upper (third) and lower (first) quartiles of the value ranges are indicated by the box ends, and the whiskers indicate the highest and lowest observations. Means having the same letters are not significantly different at $\alpha = 0.05$.



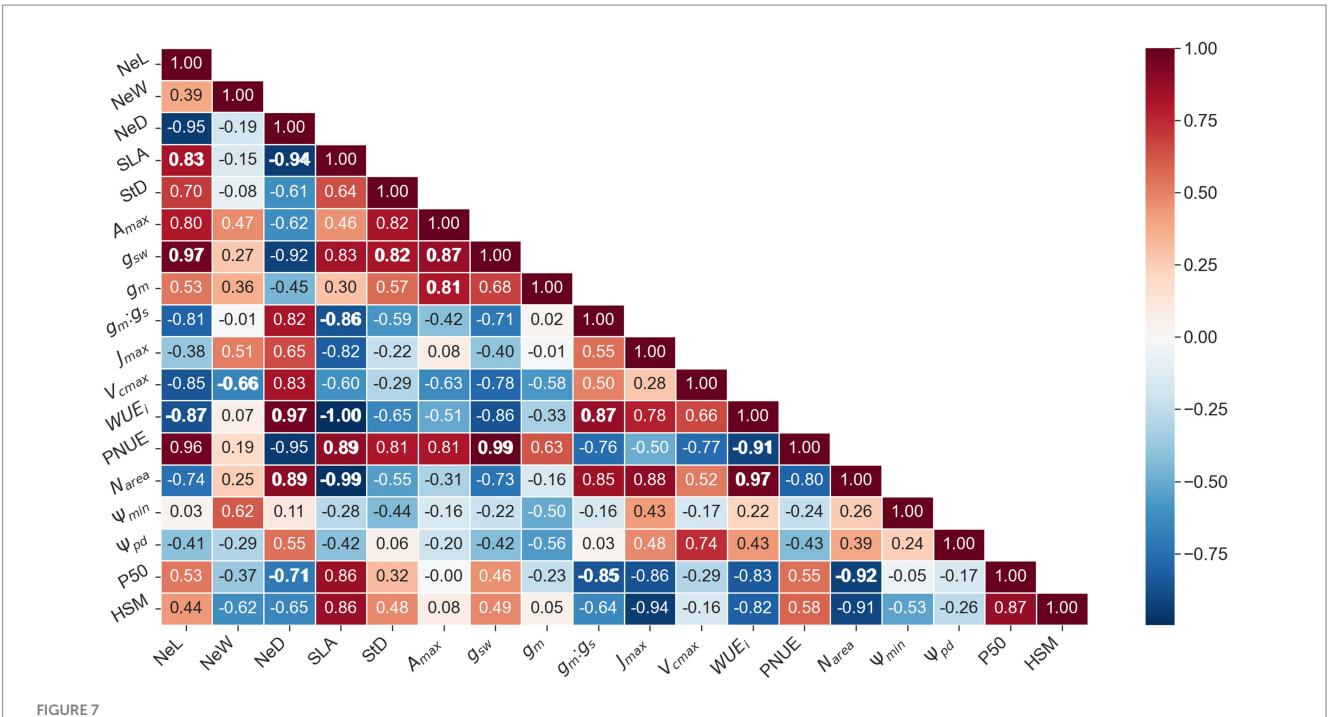
Discussion

We assessed key structural, morphological, and physiological characteristics of eastern white pine and Himalayan blue pine hybrids with varying levels of eastern white pine parentage. Our results showed that Himalayan blue pine and eastern white pine differed considerably in needle length, needle mass density, and *SLA*. As expected, our results revealed that these key traits in the hybrid progeny became more similar to those of the eastern white pine as its parentage increased (Figure 3). The traits of the second-generation backcrosses with 87.5% eastern white pine parentage were very similar to those of the eastern white pine. The

successful recovery of structural, morphological, and physiological traits of eastern white pine in the hybrid progeny through backcrossing has validated Ontario's breeding strategy (Lu and Derbowka, 2009) to enhance blister rust resistance while retaining desirable characteristics of eastern white pine.

Needle morphological characteristics

Eastern white pine needles were almost half the length of the blue pine. Furthermore, our results revealed that needle length variation



Heatmap of correlation between needle morphophysiology and xylem-related traits. The values in the grid are the Spearman correlation coefficients (r values). The red color indicates a positive correlation, and the blue color indicates a negative correlation. r values of correlations with p values ≤ 0.05 are bolded. (n = 5). Nel., Needle length; SLA, specific leaf area; NeD, needle density; StD, stomatal density; A_{max} , light-saturated photosynthetic rate; g_{sw} stomatal conductance for water; g_m , mesophyll conductance; g_m : g_s , the g_m to g_s ratio; V_{cmax} , the maximum rate of carboxylation; J_{max} , the rate of electron transport; WUE_μ intrinsic water use efficiency; PNUE, Photosynthetic nitrogen use efficiency; N_{area} , Leaf nitrogen in area basis; Midday water potential in dry period; P redawn water potential in dry period; P so, cavitation resistance; HSM, xylem hydraulic safety margin.

among hybrids is linearly related to eastern white pine parentage (Figure 5). This difference in needle length may be the cause of the observed high difference in SLA and needle density between the two species and the strong negative correlation between needle density and SLA (Figure 7). Needle morphology is involved in cold adaptation for several conifer species (Körner et al., 1989; Rajashekar and Burke, 1996; Jankowski et al., 2017). Cold-adapted species or populations generally have shorter and more compact needles, resulting from a substantial investment in structural tissue such as thicker cell walls, more epidermal cells, and wider resin ducts (Jankowski et al., 2017; Niinemets, 2016; Niinemets, 2001). This structure results in greater tissue density and lower SLA (Niinemets, 2001; Poorter et al., 2009). Our results showed a decrease in needle length and SLA, and an increase in needle density of hybrid pine with increasing eastern white pine parentage, indicating that frost tolerance of eastern white pine hybrids is proportional to eastern white pine parentage. Our results align with observations of Lu and Sinclair (2006), who found a positive correlation between eastern white pine parentage and frost tolerance in hybrid progeny. Our results indicate that progressive backcrossing of hybrids with eastern white pine helped recover frost resistance and support the expectation for a high degree of morphophysiological similarity between the third-generation backcrosses and eastern white pine.

Water potential and xylem vulnerability to cavitation

Midday needle water potential (Ψ_{md}), which ranged from -1.2 to -1.5 MPa in wet and dry conditions, respectively, is consistent with

previous findings for eastern white pine (Urli et al., 2023; Asbjornsen et al., 2021; Fulton, 2014). The small adjustment in Ψ_{md} (less than 0.5 MPa) in response to soil drying, a typical isohydric pattern of eastern white pine, has been reported by other studies (Asbjornsen et al., 2021; Urli et al., 2023; Koc et al., 2022). The Ψ_{md} and Ψ_{pd} , of blue pine and hybrids were similar to those of the eastern white pine. Furthermore, eastern white pine parentage did not affect hybrid pines' needle water potential, suggesting that hybrid pine should have the same physiological strategy to cope with drought. We found no correlation between predawn water potential (Ψ_{pd}) and midday water potential during dry period (Ψ_{min}), which could be due to isohydric characteristic of eastern white pine and its hybrids. Isohydric species tend to limit midday water potential to a specific range, regardless of predawn measurements under moderate stress conditions (Martínez-Vilalta et al., 2014; Guo et al., 2020).

Few studies investigated xylem vulnerability to cavitation in white and blue pines. Reported P50 values for eastern white pine ranged from -5.25 MPa (Asbjornsen et al., 2021) for trees growing at the southern edge of the species natural range in Durhan, NH, USA, using the centrifuge method, to -3.5 MPa (Urli et al., 2023; Song et al., 2021) in the south of Quebec, Canada using the bench dehydration method. Our P50 values were higher than those reported for eastern white pine. These differences were likely due to methods used to build the vulnerability curves. The P50 for blue pine was close to -3 MPa, lower than the eastern white pine, suggesting that blue pine is slightly more resistant to cavitation than eastern white pine. The hybrids were also more resistant to cavitation than eastern white pine. In addition, the higher hydraulic safety margin observed for hybrids compared to eastern white pine

should allow for increased drought tolerance. The resistance to drought-induced cavitation (P50) is strongly related to the tracheid dimension for most boreal conifer species, and collectively, lower P50 is associated with greater wood density (Hacke et al., 2015). Lu and Sinclair (2006) reported a decrease in wood density with an increase in eastern white pine parentage, suggesting that the P50 variation pattern observed in our study is likely linked to the observed variation in wood density among the two pines and hybrids. Based on the well-documented physiological coordination between needle stomatal and mesophyll conductance and needle hydraulic conductance (Flexas et al., 2013; Wang et al., 2019), one might expect a negative relationship between P50 and stomatal and mesophyll conductance (g_{sw}) , since greater embolism resistance (i.e., higher P50) is associated with reduced xylem hydraulic conductance. However, we did not observe this expected correlation in our study. This may be explained by the fact that total needle hydraulic conductance is determined not only by xylem hydraulic conductance but also by extravascular hydraulic conductance (Wang et al., 2019). Extravascular pathways can decouple xylem vulnerability to cavitation and needle hydraulic conductance. Therefore, while P50 provides valuable insight into embolism resistance, it may not fully capture the hydraulic limitations that influence stomatal regulation and photosynthetic activity in hybrid pines.

Photosynthetic-related traits

Needle physiology data were almost non-existent for Himalayan blue pine and the results of our study provide an opportunity to assess the physiological proximity between the two species. The light-saturated photosynthetic rate (A_{max}) was similar among the two pine species, and their hybrids. The observed variation in A_{max} was strongly related to g_{sw} and g_m but not to V_{cmax} and J_{max} . The little variation in V_{cmax} despite the high N_{area} for eastern white pine might be explained by a greater investment of needle nitrogen in structural tissues (proxied by a decrease in SLA) for frost resistance.

The differences in SLA, N_{area} and g_{sw} between the two species and their hybrids (Table 2) contributed to the observed trade-off between photosynthetic nitrogen use efficiency (PNUE) and intrinsic water use efficiency (WUE_i). However, this difference should not limit the fitness of hybrids under boreal conditions. On the contrary, it should enhance the tolerance of hybrids to frost and drought conditions.

Water-use efficiency index (WUE_i) is a crucial trait for the survival of conifer seedlings during the establishment stage particularly if they are subject to the soil water deficit (Livingston and Black, 1987; Sun et al., 1996). Water use efficiency is a complex trait which is influenced by various physiological and morphological characteristics, including stomatal density and structure, mesophyll conductance, stomatal conductance, their ratio ($g_m:g_{sw}$), and cuticle and epicuticular waxes (Flexas et al., 2016; Fanourakis et al., 2014; Petrík et al., 2024; Israel et al., 2021). Our findings indicate that after two backcrosses, the hybrids were able to nearly match the WUE_i of eastern white pine, which suggests that these hybrid pines could provide greater resilience to drought conditions in boreal forest environments. We observed no correlation between WUE_i and

stomatal density or stomatal conductance (g_{sw}), and a positive correlation with g_m : g_{sw} ratio suggesting that the observed variations in WUE_i may be linked to stomatal size, cuticle properties, or epicuticular waxes and the balance between g_s and g_m .

Across taxa, SLA correlated positively with mesophyll conductance (Niinemets et al., 2009) Unexpectedly, our results indicated a similar mesophyll conductance among the two pine species and their hybrid despite the substantial variation in SLA; one explanation may be the contribution of aquaporin to the movement of CO_2 through the mesophyll at high needle nitrogen content (Evans, 2021). Also, needle hydraulic conductance is a contributing factor to observed variation in g_m (Flexas et al., 2013). The absence of correlation between mesophyll conductance (g_m) and needle density and P50 in our study suggests contrasting patterns of xylem and outside the xylem (extra-xylary) hydraulic conductance within the needle. Analyzing the needle anatomy—such as the surface area of mesophyll cells, the thickness of mesophyll cell walls, and the diameter of tracheids—as well as the distinct roles of xylem and extra-xylary pathways in overall needle hydraulic conductance might help shed light on this matter.

In summary, our results support the effectiveness of backcrossing to recover desirable morphophysiological traits of eastern white pine in its hybrids with Himalayan blue pine. Producing third-generation backcrosses will likely help achieve the objectives of Ontario's breeding program for blister rust resistance. This study has covered a small number of families from each hybrid. Examining those traits across more families at different site conditions would be more desirable and will be the focus of future planned studies.

Data availability statement

The raw data supporting the conclusions of this article will be made available by the authors, without undue reservation.

Author contributions

LB: Conceptualization, Data curation, Formal analysis, Methodology, Writing – original draft, Writing – review & editing. RE: Conceptualization, Methodology, Visualization, Writing – review & editing. PL: Conceptualization, Funding acquisition, Project administration, Resources, Supervision, Writing – review & editing.

Funding

The author(s) declare that financial support was received for the research and/or publication of this article. This study was funded by the Ontario Ministry of Natural Resource (OMNR).

Acknowledgments

The authors thank Drs. C. Heimburger and L. Zsuffa, former OMNR geneticists, for initiating this breeding program, the authors thank B. Sinclair, D. Derbowka, T. Boult, and S. Blake for their assistance in trial establishment and Bruna Schuab and Olivia Rodrigo,

for laboratory assistance. The authors are grateful to Gillian Muir for providing comments and editorial assistance on the manuscript.

Conflict of interest

The authors declare that the research was conducted in the absence of any commercial or financial relationships that could be construed as a potential conflict of interest.

Generative AI statement

The authors declare that no Gen AI was used in the creation of this manuscript.

Any alternative text (alt text) provided alongside figures in this article has been generated by Frontiers with the support of artificial intelligence and reasonable efforts have been made to ensure accuracy, including review by the authors wherever possible. If you identify any issues, please contact us.

References

Asbjornsen, H., Mcintire, C. D., Vadeboncoeur, M. A., Jennings, K. A., Coble, A. P., and Berry, Z. C. (2021). Sensitivity and threshold dynamics of *Pinus strobus* and *Quercus* spp. in response to experimental and naturally occurring severe droughts. *Tree Physiol.* 41, 1819–1835. doi: 10.1093/treephys/tpab056

Blada, I. (2004). Genetic variation in growth and blister-rust resistance in a *Pinus strobus* x *P. wallichiana* hybrid population. *Silvae Genet.* 53, 33–41. doi: 10.1515/sg-2004-0006

Cochard, H., Damour, G., Bodet, C., Tharwat, I., Poirier, M., and Améglio, T. (2005). Evaluation of a new centrifuge technique for rapid generation of xylem vulnerability curves. *Physiol. Plant.* 124, 410–418. doi: 10.1111/j.1399-3054.2005.00526.x

Dang, Q.-L., Margolis, H. A., Coyea, M. R., Sy, M., and Collatz, G. J. (1997). Regulation of branch-level gas exchange of boreal trees: roles of shoot water potential and vapor pressure difference. *Tree Physiol.* 17, 521–535. doi: 10.1093/treephys/17.8-9.521

Delzon, S., and Cochard, H. (2014). Recent advances in tree hydraulics highlight the ecological significance of the hydraulic safety margin. *New Phytol.* 203, 355–358. doi: 10.1111/nph.12798

Delzon, S., Douthe, C., Sala, A., and Cochard, H. (2010). Mechanism of water-stress induced cavitation in conifers: bordered pit structure and function support the hypothesis of seal capillary-seeding. *Plant Cell Environ.* 33, 2101–2111. doi: 10.1111/j.1365-3040.2010.02208.x

Ethier, G. J., and Livingston, N. J. (2004). On the need to incorporate sensitivity to Co2 transfer conductance into the Farquhar–von caemmerer–berry leaf photosynthesis model. *Plant Cell Environ.* 27, 137–153. doi: 10.1111/j.1365-3040.2004.01140.x

Ethier, G. J., Livingston, N. J., Harrison, D. L., Black, T. A., and Moran, J. A. (2006). Low stomatal and internal conductance to Co2 versus rubisco deactivation as determinants of the photosynthetic decline of ageing evergreen leaves. *Plant Cell Environ.* 29, 2168–2184. doi: 10.1111/j.1365-3040.2006.01590.x

Evans, J. R. (2021). Mesophyll conductance: walls, membranes and spatial complexity. New Phytol. 229, 1864–1876. doi: 10.1111/nph.16968

Fanourakis, D., Giday, H., Milla, R., Pieruschka, R., Kjaer, K. H., Bolger, M., et al. (2014). Pore size regulates operating stomatal conductance, while stomatal densities drive the partitioning of conductance between leaf sides. *Ann. Botany* 115, 555–565. doi: 10.1093/aob/mcu247

Farquhar, G. D., Von Caemmerer, S., and Berry, J. A. (1980). A biochemical model of photosynthetic Co2 assimilation in leaves of C3 species. *Planta* 149, 78–90. doi: 10.1007/BF00386231

Flexas, J., Díaz-Espejo, A., Conesa, M. A., Coopman, R. E., Douthe, C., Gago, J., et al. (2016). Mesophyll conductance to Co2 and rubisco as targets for improving intrinsic water use efficiency in C3 plants. *Plant Cell Environ*. 39, 965–982. doi: 10.1111/pce.12622

Flexas, J., Scoffoni, C., Gago, J., and Sack, L. (2013). Leaf mesophyll conductance and leaf hydraulic conductance: an introduction to their measurement and coordination. *J. Exp. Bot.* 64, 3965–3981. doi: 10.1093/jxb/ert319

Fulton, M. (2014). Hydraulic limitation on maximum height of $Pinus\ strobus$ trees in northern Minnesota, USA. Trees 28, 841–848. doi: 10.1007/s00468-014-0996-z

Publisher's note

All claims expressed in this article are solely those of the authors and do not necessarily represent those of their affiliated organizations, or those of the publisher, the editors and the reviewers. Any product that may be evaluated in this article, or claim that may be made by its manufacturer, is not guaranteed or endorsed by the publisher.

Supplementary material

The Supplementary material for this article can be found online at: https://www.frontiersin.org/articles/10.3389/ffgc.2025.1645556/full#supplementary-material

SUPPLEMENTARY FIGURE 1

Photosynthetic light response curve of eastern white pine (Parentage of *P. strobus* = 100%), interspecific hybrid pine with 87.5% eastern white pine parentage (Parentage of *P. strobus* = 87.5%), and Himalayan blue pine (Parentage of *P. strobus* = 0%).

Ghimire, B., Lee, C., Yang, J., and Heo, K. (2015). Comparative leaf anatomy of native and cultivated *Pinus* (Pinaceae) in Korea: implication for the subgeneric classification. *Plant Syst. Evol.* 301, 531–540. doi: 10.1007/s00606-014-1090-0

Guo, J. S., Hultine, K. R., Koch, G. W., Kropp, H., and Ogle, K. (2020). Temporal shifts in iso/anisohydry revealed from daily observations of plant water potential in a dominant desert shrub. *New Phytol.* 225, 713–726. doi: 10.1111/nph.16196

Hacke, U. G., Lachenbruch, B., Pittermann, J., Mayr, S., Domec, J.-C., and Schulte, P. J. (2015). "The hydraulic architecture of conifers" in Functional and ecological xylem anatomy. ed. U. Hacke (Cham: Springer International Publishing).

Heimburger, C. (1962). Breeding for disease resistance in forest trees. For. Chron. 38, 356-362. doi: 10.5558/tfc38356-3

Heimburger, C. (1972). Relative blister rust resistance of native and introduced white pines in North America. In: Biology of Rust Resistance in Forest Trees, Misc. Publ. 1221, USDA For. Serv., Washington, DC, pp. 257–269.

Houminer, N., Riov, J., Moshelion, M., Osem, Y., and David-Schwartz, R. (2022). Comparison of morphological and physiological traits between *Pinus brutia*, Pinus halepensis, and their vigorous F1 hybrids. *Forests* 13:1477. doi: 10.3390/f13091477

Israel, W. K., Watson-Lazowski, A., Chen, Z.-H., and Ghannoum, O. (2021). High intrinsic water use efficiency is underpinned by high stomatal aperture and guard cell potassium flux in C3 and C4 grasses grown at glacial Co2 and low light. *J. Exp. Bot.* 73, 1546–1565. doi: 10.1093/jxb/erab477

Jankowski, A., Wyka, T. P., Żytkowiak, R., Nihlgård, B., Reich, P. B., and Oleksyn, J. (2017). Cold adaptation drives variability in needle structure and anatomy in *Pinus sylvestris* L. along a 1,900 km temperate–boreal transect. *Funct. Ecol.* 31, 2212–2223. doi: 10.1111/1365-2435.12946

Keng, H., Elbert, L., and Little, J. (1961). Needle characteristics of hybrid pines. Silvae Genet. 10, 131–146.

Klein, T., Yakir, D., Buchmann, N., and Grünzweig, J. M. (2014). Towards an advanced assessment of the hydrological vulnerability of forests to climate change-induced drought. *New Phytol.* 201, 712–716. doi: 10.1111/nph.12548

Koc, I., Nzokou, P., and Cregg, B. (2022). Biomass allocation and nutrient use efficiency in response to water stress: insight from experimental manipulation of balsam fir, concolor fir and white pine transplants. New For. 53, 915–933. doi: 10.1007/s11056-021-09894-7

Körner, C., Neumayer, M., Menendez-Riedl, S. P., and Smeets-Scheel, A. (1989). Functional morphology of mountain plants 1 1dedicated to prof. H. Meusel, on the occasion of his 80th birthday. *Flora* 182, 353–383. doi: 10.1016/S0367-2530(17)30426-7

Lilly, C. J., Will, R. E., and Tauer, C. G. (2012). Physiological and morphological attributes of shortleaf × loblolly pine F1 hybrid seedlings: is there an advantage to being a hybrid? *Can. J. For. Res.* 42, 238–246. doi: 10.1139/x11-180

Livingston, N. J., and Black, T. A. (1987). Water stress and survival of three species of conifer seedlings planted on a high elevation south-facing clear-cut. *Can. J. For. Res.* 17, 1115–1123. doi: 10.1139/x87-170

Long, S. P., and Bernacchi, C. J. (2003). Gas exchange measurements, what can they tell us about the underlying limitations to photosynthesis? Procedures and sources of error. *J. Exp. Bot.* 54, 2393–2401. doi: 10.1093/jxb/erg262

- Lu, P., Colombo, S. J., and Sinclair, R. W. (2007). Cold hardiness of interspecific hybrids between Pinus strobus and *P. wallichiana* measured by post-freezing needle electrolyte leakage. *Tree Physiol.* 27, 243–250. doi: 10.1093/treephys/27.2.243
- Lu, P., and Derbowka, D. (2009). Breeding eastern white pine for blister rust resistance: a review of progress in Ontario. *For. Chron.* 85, 745–755. doi: 10.5558/tfc85745-5
- Lu, P., and Sinclair, R. W. (2006). Survival, growth and wood specific gravity of interspecific hybrids of Pinus strobus and *P. wallichiana* grown in Ontario. *For. Ecol. Manag.* 234, 97–106. doi: 10.1016/j.foreco.2006.06.027
- Lu, P., Sinclair, R. W., Boult, T. J., and Blake, S. G. (2005). Seedling survival of Pinus strobus and its interspecific hybrids after artificial inoculation of *Cronartium ribicola*. *For. Ecol. Manag.* 214, 344–357. doi: 10.1016/j.foreco.2005.04.024
- Martínez-Vilalta, J., Poyatos, R., Aguadé, D., Retana, J., and Mencuccini, M. (2014). A new look at water transport regulation in plants. *New Phytol.* 204, 105–115. doi: 10.1111/nph.12912
- Niinemets, Ü. (2001). Global-scale climatic controls of leaf dry mass per area, density, and thickness in trees and shrubs. *Ecology* 82, 453–469. doi: 10.1890/0012-9658(2001)082[0453:GSCCOL]2.0.CO;2
- Niinemets, Ü. (2016). Does the touch of cold make evergreen leaves tougher? *Tree Physiol.* 36, 267–272. doi: 10.1093/treephys/tpw007
- Niinemets, Ü., Díaz-Espejo, A., Flexas, J., Galmés, J., and Warren, C. R. (2009). Role of mesophyll diffusion conductance in constraining potential photosynthetic productivity in the field. *J. Exp. Bot.* 60, 2249–2270. doi: 10.1093/jxb/erp036
- Niinemets, Ü., Sonninen, E., and Tobias, M. (2004). Canopy gradients in leaf intercellular Co2 mole fractions revisited: interactions between leaf irradiance and water stress need consideration. *Plant Cell Environ.* 27, 569–583. doi: 10.1111/j.1365-3040.2003.01168.x
- Niinemets, Ü., and Tenhunen, J. D. (1997). A model separating leaf structural and physiological effects on carbon gain along light gradients for the shade-tolerant species *Acer saccharum*. *Plant Cell Environ*. 20, 845–866. doi: 10.1046/j.1365-3040.1997.d01-133.x
- Nobis, M. P., Christopher, T., and Roth-Nebelsick, A. (2012). Latitudinal variation in morphological traits of the genus *Pinus* and its relation to environmental and phylogenetic signals. *Plant Ecol. Divers.* 5, 1–11. doi: 10.1080/17550874.2012.687501
- Onoda, Y., Wright, I. J., Evans, J. R., Hikosaka, K., Kitajima, K., Niinemets, Ü., et al. (2017). Physiological and structural tradeoffs underlying the leaf economics spectrum. *New Phytol.* 214, 1447–1463. doi: 10.1111/nph.14496
- Pammenter, N. W., and Van Der Willigen, C. (1998). A mathematical and statistical analysis of the curves illustrating vulnerability of xylem to cavitation. *Tree Physiol.* 18, 589–593. doi: 10.1093/treephys/18.8-9.589
- Parker, W. (2008). Ecology and management of eastern white pine in the Lake Abitibi (3E) and Lake Temagami (4E) ecoregions of Ontario, vol. 71. Sault Ste. Marie, Ontario Canada: Ontario Ministry of Natural Resources.
- Patton, R. F. (1966). "Interspecific hybridization in breeding for white pine blister rust resistance" in Breeding Pest-resistant trees. eds. H. D. Gerhold, E. J. Schreiner, R. E. Mcdermott and J. A. Winieski (Oxford, London: Pergamon Press). Available online at: https://api.pageplace.de/preview/DT0400.9781483158389_A23874508/pteview-9781483158389_A23874508.pdf

- Petrík, P., Petek-Petrík, A., Lamarque, L. J., Link, R. M., Waite, P.-A., Ruehr, N. K., et al. (2024). Linking stomatal size and density to water use efficiency and leaf carbon isotope ratio in juvenile and mature trees. *Physiol. Plant.* 176:e14619. doi: 10.1111/ppl.14619
- Pitt, D. G., Meyer, T., Park, M., Macdonald, L., Buscarini, T., and Thompson, D. G. (2006). Application of slow-release tablets to enhance white pine regeneration: growth response and efficacy against white pine blister rust. *Can. J. For. Res.* 36, 684–698. doi: 10.1139/x05-278
- Poorter, H., Niinemets, Ü., Poorter, L., Wright, I. J., and Villar, R. (2009). Causes and consequences of variation in leaf mass per area (Lma): a meta-analysis. *New Phytol.* 182, 565–588. doi: 10.1111/j.1469-8137.2009.02830.x
- Rajashekar, C. B., and Burke, M. J. (1996). Freezing characteristics of rigid plant tissues (development of cell tension during extracellular freezing). *Plant Physiol.* 111, 597–603. doi: 10.1104/pp.111.2.597
- Reich, P. B., Wright, I. J., Cavender-Bares, J. M., Craine, J. M., Oleksyn, J., Oleksyn, J., et al. (2003). The evolution of plant functional variation: traits, spectra, and strategies. *Int. J. Plant Sci.* 164, S143–S164. doi: 10.1086/374368
- Rodriguez-Dominguez, C. M., Forner, A., Martorell, S., Choat, B., Lopez, R., Peters, J. M. R., et al. (2022). Leaf water potential measurements using the pressure chamber: synthetic testing of assumptions towards best practices for precision and accuracy. *Plant Cell Environ.* 45, 2037–2061. doi: 10.1111/pce.14330
- Rosner, S. (2017). Wood density as a proxy for vulnerability to cavitation: size matters. J. Plant Hydraul. 4:e001. doi: 10.20870/jph.2017.e001
- Song, Y., Poorter, L., Horsting, A., Delzon, S., and Sterck, F. (2021). Pit and tracheid anatomy explain hydraulic safety but not hydraulic efficiency of 28 conifer species. *J. Exp. Bot.* 73, 1033–1048. doi: 10.1093/jxb/erab449
- Spaulding, P. (1922). Investigations of the white-pine blister rust. Bulletin No. 957. U.S. Department of Agriculture, Washington, D.C. $100~\rm p.$
- Sun, J., Feng, Z., Leakey, A. D. B., Zhu, X., Bernacchi, C. J., and Ort, D. (2014). Inconsistency of mesophyll conductance estimate causes the inconsistency for the estimates of maximum rate of rubisco carboxylation among the linear, rectangular and non-rectangular hyperbola biochemical models of leaf photosynthesis—a case study of Co2 enrichment and leaf aging effects in soybean. *Plant Sci.* 226, 49–60. doi: 10.1016/j.plantsci.2014.06.015
- Sun, Z. J., Livingston, N. J., Guy, R. D., and Ethier, G. J. (1996). Stable carbon isotopes as indicators of increased water use efficiency and productivity in white spruce (*Picea glauca* (Moench) Voss) seedlings. *Plant Cell Environ*. 19, 887–894. doi: 10.1111/j.1365-3040.1996.tb00425.x
- Urli, M., Périé, C., Thiffault, N., Coyea, M. R., Pepin, S., Logan, T., et al. (2023). Experimental drier climates affect hydraulics and induce high mortality of seedlings of three northern conifer species. *For. Ecol. Manag.* 544:121127. doi: 10.1016/j.foreco.2023.121127
- Wang, N., Palmroth, S., Maier, C. A., Domec, J.-C., and Oren, R. (2019). Anatomical changes with needle length are correlated with leaf structural and physiological traits across five species. *Plant Cell Environ.* 42, 1690–1704. doi: 10.1111/pce.13516
- Wendel, G., and Smith, H. (1990). Silvics of North America. Vol 1: Conifers, vol. 654. Washington, DC: Washington DCUS Forest Service, Agriculture Handbook. Available online at: https://www.srs.fs.usda.gov/pubs/misc/ag_654_vol1.pdf